VOL. 14, NO. 7, APRIL 2019 ISSN 1819-6608
ARPN Journal of Engineering and Applied Sciences
©2006-2019 Asian Research Publishing Network (ARPN). All rights reserved.

www.arpnjournals.com

# EFFECT OF AGING ON THE DISSIPATED ENERGY FOR EVALUATING FATIGUE BEHAVIOR OF IRAQI ASPHALT BINDERS

Alaa H. Abed
Civil Engineering Department, Al-Nahrain University, Baghdad, Iraq
E-Mail: alaa.abed@eng.nahrainuniv.edu.iq


## ABSTRACT

Many researches used dissipated energy approach to find the changing of the asphalt binder properties through repeated cyclic loading with accumulation of damage. In this research time-sweep and stress - sweep tests were used to simulate fatigue phenomenon for the different production refineries of Iraqi asphalt binders (Nasiriya, Daurah and Basrah) by applying repeated cyclic load of strain or stress at chosen loading frequency and temperatures. The asphalt binders were aged by rolling thin film oven for simulating influence of oxidation in the mixing and compaction of HMA, and pressure aging vessel to represent long term oxidation life. All the tests were conducted at 10 Hz at intermediate temperatures and 3 percent of strain that closest to the HMA mixture beam fatigue behavior [1], different mathematical models were founded to represent relation of the dissipated energy ratio and fatigue life at constant stress value (150 and 200) kPa for RTFO aging and 300, 350 kPa for PAV aging. It was found that fatigue life of Al-Nasiriya asphalt binder more than Daurah and Basrah by 67%, 187% respectively for long term aging. In general, it was noticed that the stiffness modulus (*G*)* values accelerated and quickly reached to the failure criteria, as decreased about 55% of the original G* value.


**Keywords:** dissipated energy, fatigue life, time-sweep, stress-sweep, control stress, control strain.

## 1. INTRODUCTION

Superpave used shear modulus and viscosity variables(G*.sinδ)to represent the fatigue efficiency of the asphalt, which is refer the total dissipated energy through cyclic loading within the linear viscoelastic scope before damage take place [1]. Fatigue is considered one of the major complexed failure occur in the HMA pavement. Fatigue cracks begin and propagate through the asphalt binder, so, an asphalt binder associated failure should be restraint in the asphalt specification. A large number of researchers confirm that it is a mixture issue, however, many researchers concluded that it is a pavement structural issue [2]. The fatigue parameter G*. sinδ which obtained by Superpave performance grade for asphalt binder measured by applying small strain in the linear viscoelastic range, that leads to lack correlation between fatigue of asphalt binder and mixture [1]. Dissipated energy approach is introduced by [3] to show the influence of repeated cyclic loading on the asphalt binder properties through changing of dissipated energy with the accumulation of damage.

## 2. OBJECTIVE

The objective of this research is to estimate the effectiveness of applying dissipated energy method for predicating the fatigue behavior modes of the different local asphalt binders produce in Iraq, also, this study is focused on the changing rate of the dissipated energy for RTFO and PAV aging of the selected local asphalt binders using controlled-strain cyclic tests.

## 3. DISSIPATED ENERGY METHOD

The main theory used for explaining the fatigue failure in HMA are decreasing in the initial stiffness by 50 percent. These theory does not provide an appropriate indication of the level and the development of failure in the asphalt binder in terms of variation in mechanistic behavior under loading formula. To understand the action of aging in the asphalt binder on the fatigue execution, and to be fit the analysis of reliable fatigue conductance, dissipated energy method has been used in this study to give a better indicator to simulate fatigue behavior with the rate of change in the dissipated energy for each cycling loading.

This approach is presented by [4]to calculate the rate of change for dissipated energy as follows:

$$\text{Actual } w_{i=}\pi_i \sigma_i \varepsilon_i \sin\delta$$

$$\text{Calculating } w_{i=}\pi_i \frac{{\sigma_i}^2}{G^*} \sin\delta$$

$$\sum_{i=1}^{n} w_i = nw_c$$

$$\text{DER} = \frac{\sum_{i=1}^{n} w_i}{w_n}$$

| | |
|---|---|
| $W_i$ | = dissipated energy for each load cycle, |
| $\sigma_i$ | = stress value ati cycle, |
| $\varepsilon_i$ | = the strain value at icycle, |
| δ | = phase angle difference between the stress and strain signs, |
| Wc | = accumulated dissipated energy for n cycles, |
| DER | = dissipated energy ratio |
| n | = total of cyclic numbers, and |
| $W_n$ | = the dissipated energy at n cycle. |

A large number of studies are used a different way to evaluate fatigue behavior depending on the changing of the dissipated energy of asphalt binder, [5] and [6] were illustrated that the dissipated energy access gives a good dependable estimation way for classifying asphalt binder behaviors. Figure-1 shows snap for the EXCEL sheet which was used for the calculating and

©2006-2019 Asian Research Publishing Network (ARPN). All rights reserved.


analysis rate of change in the dissipated energy to represent fatigue behavior.

## 4. MATERIALS AND TESTING

### 4.1 Materials

Four types of local neat asphalt binder's product from three oil refiners (Daurah-Basrah - Nasiritah) with two performance grade PG (64-16) and PG (58-22) were used in this research, these types of asphalt binders extremely have been used in Iraq. The asphalt binders were subjected to short-term aging using (RTFO) oven to simulate the short-term aging operation through mixing and compaction for pavement construction, then subjected to pressure aging vessel to simulate long term aging through long service life.

### 4.2 Time-sweep test

The time-sweep experiment is considered major test to assess the fatigue action of the asphalt binder. The test can be carried out by the dynamic shear rheometer through a small amount of time. This technique can give dependable results that correlate well with HMA showing (Bahia, Hanson et al. 2001). The DSR was used to find time-sweep effort. The test provides shear frequently cycling of strain or stress loading at elected loading frequency and temperatures.

Effects of temperature, frequency, strain, and stress conditions were measured. [7] Introduced details of the binder fatigue tests. The time sweep test technique applies a frequent cyclic sinusoidal loading on an asphalt binder sample at a constant amplitude, temperature and frequency, at failure fatigue life ($N_f$) can be found by time sweep test using control stress or control strain modes [8].

It can be seen that is a notable difference in the magnitude of dissipated energy at fatigue failure for each cycle, especially when the fatigue damage progresses from crack initiation to crack development. The term (Np) which utilized in this technique to indicate transition of fatigue crack from initiation to development (propagation) through fatigue test measured, which is independent to loading mode. Figure-2 shows relation between shear complex modulus $G^*$ and number of cycles for Nasiriya PG(64-16), Daurah PG(64-16), Daurah PG(58-22), Basrah PG(64-16) at 200 kPa, 28 $^oC$, 25 $^oC$ and RTFO aging, while Figure-3 shows relation of shear complex modulus $G^*$ with number of cycles for Nasiriya PG(64-16), Daurah PG(64-16), Daurah PG(58-22), Basrah PG(64-16) at 350 kPa, 28 $^oC$, and PAV aging, as predictable, $G^*$value is decreased in relation to increase of repeating load,which point out occurrence of failure, also, it can be seen that the percentage of complex modulus increasing with aging although the shear stress testing changes from (200) to (350) kPa.

It can be seen that the energy dissipated method effectively used for evaluating local asphalt binders,due to the difficulty of locating a sharp difference of fatigue failure in the control stressor strain tests, the 20-percent difference is choosing to mark boundary of exceeds the test error that yield a confirmed demonstration of failurecumulation. Figure-4 show typical application for the amount of dissipated energy with number of cycles for Al-Nasiriya asphalt, Np represent the irrecoverable fatigue asymptote and the viscoelastic damping asymptote.

### 4.3 Stress sweep test

The fatigue phenomenon of asphalt is influenced by several operators, like temperature and magnitude of loading and frequency. In this research, various stress values were utilized to test the asphalt. Figure-5 and Figure-6 show decreasing of the shear complex modulus $G^*$ of Al Nasiriya, Daurah, and Basrah asphalt binders with applied shear stress at RTFO and PAV aging. It can be seen that increasing of applied shear stress lead to decreasing $G^*$ quickly at different aging.

## 5. MODES OF FATIGUE FAILURE FOR DIFFERENT TYPES OF LOCAL ASPHALT BINDERS

The fatigue characteristics of asphalt binder can be calculated from log-log plots of dissipated energy per cycle to fatigue life failure and by obtaining the slope band value of a of the resulting straight line, which indicates that the fatigue behavior of asphalt binder may be predicted using the following empirical power law relationship:

$$DER \quad = a \, (N_{p20})^b$$

Where
DER = dissipated energy ratio
$N_{p20}$ = percentage number of cycles that give definite indication of damage accumulation
$a$ and $b$ = fatigue parameters

Figures (7) and (8) show calculating modes of fatigue life failure for the different local asphalt binders at RTFO and PAV aging.

## 6. CONCLUSIONS

The following conclusions may be concluded in this research.

a) The percent of increases in fatigue life for Nasiriya asphalt binder to Daurah 9.5%, and 18% for Nasiriya to Basrah measured at 200 kPa- rolling thin film aging, it can be noticed that no significant differences for fatigue life through production and compaction.

b) When test asphalt binders at 300 KPa and pressure aging vessel aging, it can be found that the ratio of increasing fatigue life of Al-Nasiriya asphalt to Daurahis 67%, while it was increased by 187% for Nasiriya to Basrah.

c) Different mathematical models obtained to simulated relation between dissipated energy and fatigue life for

©2006-2019 Asian Research Publishing Network (ARPN). All rights reserved.


Iraqi asphalt production refineries at constant stress and RTFO, PAV aging.

d) It can be seen that *G**value accelerated and rapidly approach to the failure specification, as decreased about 55% of the original G* value.

## REFERENCES


[1] Bahia H., Hanson D., Zeng M., Zhai H., Kharti M., Anderson R. 2001. NCHRP report 459. Characterization of Modified Asphalt Binders in Superpave Mix Design. National Academy Press, Washington, DC.

[2] Bahia H.U., Anderson. D.A. 1995. The New Proposed Rheological Properties: Why Are They Required and How Do They Compare to Conventional Properties, of Asphalt Cement Binder”. American Society for Testing and Materials. 1-27.

[3] Pronk A.C. 1995. Evaluation of the Dissipated Energy Concept for the Interpretation of Fatigue Measurements in the Crack Initiation Phase. Road and Hydraulic Engineering Division, the Netherlands.

[4] Carpenter S.H. and M. Jansen. 1997. Fatigue Behavior under New Aircraft Loading Conditions. Aircraft/Pavement Technology, Proceedings of Airfield Pavement Conference, Seattle, WA; American Society of Civil Engineers, New York. 259-277.

[5] Ghuzlan K., Carpenter S. 2000. Energy-derived, damage-based failure criterion for fatigue testing. Transportation Research Record: Journal of the Transportation Research Board. (1723): 141-149.

[6] Al-Haddad A.H. 2015. Fatigue evaluation of Iraqi asphalt binders based on the dissipated energy and viscoelastic continuum damage (VECD) approaches. Journal of Civil Engineering and Construction Technology 6(3): 27-50.

[7] Bahia H.U., Zhai H., Bonnetti K., Kose S. 1999. Non-linear viscoelastic and fatigue properties of asphalt binders. Journal of the Association of Asphalt Paving Technologists. 68, 1-34.

[8] Anderson D.A., Christensen D.W., Bahia H.U., Dongre R., Sharma M., Antle C.E., Button J. 1994. Binder characterization and evaluation, volume 3: Physical characterization. Strategic Highway Research Program, National Research Council, Report No. SHRP-A-369.

ARPN Journal of Engineering and Applied Sciences
©2006-2019 Asian Research Publishing Network (ARPN). All rights reserved.


| | | | | | | | | | | | | | | | | | | | | | | |
|---|---|---|---|---|---|---|---|---|---|---|---|---|---|---|---|---|---|---|---|---|---|---|
| Check | | | Daura64-1t T (C) = 28 Stress (kPa) = 200 | | | | | | | | | | | | | | $N_{10}$ | 10 | $N_{20}$ | 20 | | |
| 72.25434 | | | $R_{de} = R_c+a_1(N-N_c)+S(a_2-a_1)\ln\{1+\exp[(N-N_c)/S]\}$ | | | | | | | | | | | | | | 7674 | 0 | 9310 | 0 | | |
| | $R'_{de}(0)$ | $R_{de}(0)$ | $R_c$ = | $N_c$ = | S= | $a_1$ = | $a_2$ = | $R^2$ = | $N_p$ = | $N_{10}$ = | $N_{20}$ = | $N_{p2}$ = | | | | | 7674 | 7674 | 9310 | 9310 | | |
| | 1.0000 | 0.0000 | 9434 | 9260 | 2.209E+03 | 1.0151 | 0.0000 | 0.2313 | 7451 | 7674 | 9310 | 9434 | | | | | 7620.00 | 9.78 | 9433.92 | 19.38 | | |
| | | | | | | | | | | | | | | | | | 7680.00 | 10.03 | 9300.00 | 20.05 | | |
| Calculation | | | | | | | Average | | | | | | | | Fit | | Percentage | | Area | | Cl | |
| | | Test 2 | | | | | | | | | | | | | | | | | | | | |
| Cum DE | Rde | Cycle | Dis E | Inc DE | Cum DE | Rde | Time | G* | Phase Angle | Cycle | Dis E | Inc DE | Cum DE | Rde | Rde | $d(Rde)^2$ | N | % | Inc | A | N | Tangent |
| ($J/m^3$) | | | ($J/m^3$) | ($J/m^3$) | ($J/m^3$) | | (s) | (Pa) | (deg) | | ($J/m^3$) | ($J/m^3$) | ($J/m^3$) | 7451.36 | Fit | | | | | | | 1 |
| | | | | | | | | | | | | | | | z | 9.96E+05 | | | | | | |
| 8.00E+02 | 6.00E+01 | 60.00 | 1.33E+01 | 8.00E+02 | 8.00E+02 | 6.00E+01 | 6 | 8.12E+03 | 59.6 | 60.00 | 1.33E+01 | 8.00E+02 | 8.00E+02 | 60.00 | 59.99 | 1.50E-04 | 60.00 | 0.00 | 0.00E+00 | 0.00E+00 | 0 | 0 |
| 1.58E+03 | 1.24E+02 | 120.00 | 1.28E+01 | 7.84E+02 | 1.58E+03 | 1.24E+02 | 12 | 8.43E+03 | 59.06 | 120.00 | 1.28E+01 | 7.84E+02 | 1.58E+03 | 123.89 | 119.95 | 1.55E+01 | 120.00 | -3.24 | -1.17E+02 | -1.17E+02 | 0 | 0 |
| 2.35E+03 | 1.85E+02 | 180.00 | 1.27E+01 | 7.65E+02 | 2.35E+03 | 1.85E+02 | 18 | 8.47E+03 | 59.01 | 180.00 | 1.27E+01 | 7.65E+02 | 2.35E+03 | 184.67 | 179.89 | 2.28E+01 | 180.00 | -2.59 | -2.57E+02 | -3.73E+02 | 7451 | 7451 |
| 3.11E+03 | 2.45E+02 | 240.00 | 1.27E+01 | 7.63E+02 | 3.11E+03 | 2.45E+02 | 24 | 8.47E+03 | 59.01 | 240.00 | 1.27E+01 | 7.63E+02 | 3.11E+03 | 244.77 | 239.80 | 2.47E+01 | 240.00 | -1.99 | -2.83E+02 | -6.56E+02 | 100000 | 100000 |
| 3.88E+03 | 3.04E+02 | 300.00 | 1.27E+01 | 7.64E+02 | 3.88E+03 | 3.04E+02 | 30 | 8.46E+03 | 59.02 | 300.00 | 1.27E+01 | 7.64E+02 | 3.88E+03 | 304.48 | 299.68 | 2.30E+01 | 300.00 | -1.49 | -2.77E+02 | -9.34E+02 | 1000000 | 1000000 |
| 4.64E+03 | 3.64E+02 | 360.00 | 1.27E+01 | 7.64E+02 | 4.64E+03 | 3.64E+02 | 36 | 8.45E+03 | 59.03 | 360.00 | 1.27E+01 | 7.64E+02 | 4.64E+03 | 364.13 | 359.54 | 2.11E+01 | 360.00 | -1.15 | -2.58E+02 | -1.19E+03 | | |
| 5.41E+03 | 4.24E+02 | 420.00 | 1.28E+01 | 7.65E+02 | 5.41E+03 | 4.24E+02 | 42 | 8.44E+03 | 59.05 | 420.00 | 1.28E+01 | 7.65E+02 | 5.41E+03 | 423.53 | 419.37 | 1.74E+01 | 420.00 | -0.84 | -2.30E+02 | -1.42E+03 | | |
| 6.17E+03 | 4.83E+02 | 480.00 | 1.28E+01 | 7.66E+02 | 6.17E+03 | 4.83E+02 | 48 | 8.44E+03 | 59.06 | 480.00 | 1.28E+01 | 7.66E+02 | 6.17E+03 | 483.11 | 479.17 | 1.56E+01 | 480.00 | -0.65 | -1.99E+02 | -1.62E+03 | | |
| 6.94E+03 | 5.43E+02 | 540.00 | 1.28E+01 | 7.67E+02 | 6.94E+03 | 5.43E+02 | 54 | 8.43E+03 | 59.07 | 540.00 | 1.28E+01 | 7.67E+02 | 6.94E+03 | 542.51 | 538.93 | 1.28E+01 | 540.00 | -0.46 | -1.69E+02 | -1.79E+03 | | |
| 7.71E+03 | 6.02E+02 | 600.00 | 1.28E+01 | 7.68E+02 | 7.71E+03 | 6.02E+02 | 60 | 8.42E+03 | 59.08 | 600.00 | 1.28E+01 | 7.68E+02 | 7.71E+03 | 601.77 | 598.67 | 9.59E+00 | 600.00 | -0.29 | -1.28E+02 | -1.92E+03 | | |
| 8.48E+03 | 6.61E+02 | 660.00 | 1.28E+01 | 7.69E+02 | 8.48E+03 | 6.61E+02 | 66 | 8.41E+03 | 59.1 | 660.00 | 1.28E+01 | 7.69E+02 | 8.48E+03 | 661.04 | 658.38 | 7.07E+00 | 660.00 | -0.16 | -8.42E+01 | -2.00E+03 | | |
| 9.25E+03 | 7.20E+02 | 720.00 | 1.28E+01 | 7.70E+02 | 9.25E+03 | 7.20E+02 | 72 | 8.40E+03 | 59.11 | 720.00 | 1.28E+01 | 7.70E+02 | 9.25E+03 | 720.14 | 718.05 | 4.37E+00 | 720.00 | -0.02 | -3.54E+01 | -2.04E+03 | | |
| 1.00E+04 | 7.80E+02 | 780.00 | 1.28E+01 | 7.71E+02 | 1.00E+04 | 7.80E+02 | 78 | 8.39E+03 | 59.11 | 780.00 | 1.28E+01 | 7.71E+02 | 1.00E+04 | 779.61 | 777.69 | 3.66E+00 | 780.00 | 0.05 | 7.51E+00 | -2.03E+03 | | |
| 1.08E+04 | 8.39E+02 | 840.00 | 1.29E+01 | 7.71E+02 | 1.08E+04 | 8.39E+02 | 84 | 8.38E+03 | 59.12 | 840.00 | 1.29E+01 | 7.71E+02 | 1.08E+04 | 838.56 | 837.30 | 1.58E+00 | 840.00 | 0.17 | 5.51E+01 | -1.97E+03 | | |
| 1.16E+04 | 8.98E+02 | 900.00 | 1.29E+01 | 7.72E+02 | 1.16E+04 | 8.98E+02 | 90 | 8.38E+03 | 59.13 | 900.00 | 1.29E+01 | 7.72E+02 | 1.16E+04 | 897.95 | 896.87 | 1.16E+00 | 900.00 | 0.23 | 1.05E+02 | -1.87E+03 | | |
| 1.23E+04 | 9.57E+02 | 960.00 | 1.29E+01 | 7.73E+02 | 1.23E+04 | 9.57E+02 | 96 | 8.37E+03 | 59.14 | 960.00 | 1.29E+01 | 7.73E+02 | 1.23E+04 | 957.19 | 956.41 | 6.10E-01 | 960.00 | 0.29 | 1.46E+02 | -1.72E+03 | | |
| 1.31E+04 | 1.02E+03 | 1020.00 | 1.29E+01 | 7.73E+02 | 1.31E+04 | 1.02E+03 | 102 | 8.36E+03 | 59.14 | 1020.00 | 1.29E+01 | 7.73E+02 | 1.31E+04 | 1016.24 | 1015.91 | 1.15E-01 | 1020.00 | 0.37 | 1.97E+02 | -1.53E+03 | | |
| 1.39E+04 | 1.08E+03 | 1080.00 | 1.29E+01 | 7.74E+02 | 1.39E+04 | 1.08E+03 | 108 | 8.36E+03 | 59.15 | 1080.00 | 1.29E+01 | 7.74E+02 | 1.39E+04 | 1075.13 | 1075.37 | 5.36E-02 | 1080.00 | 0.45 | 2.59E+02 | -1.27E+03 | | |
| 1.47E+04 | 1.13E+03 | 1140.00 | 1.29E+01 | 7.75E+02 | 1.47E+04 | 1.13E+03 | 114 | 8.35E+03 | 59.16 | 1140.00 | 1.29E+01 | 7.75E+02 | 1.47E+04 | 1134.23 | 1134.79 | 3.16E-01 | 1140.00 | 0.51 | 3.19E+02 | -9.49E+02 | | |
| 1.54E+04 | 1.19E+03 | 1200.00 | 1.29E+01 | 7.76E+02 | 1.54E+04 | 1.19E+03 | 120 | 8.34E+03 | 59.16 | 1200.00 | 1.29E+01 | 7.76E+02 | 1.54E+04 | 1193.39 | 1194.17 | 6.10E-01 | 1200.00 | 0.55 | 3.72E+02 | -5.78E+02 | | |
| 1.62E+04 | 1.25E+03 | 1260.00 | 1.29E+01 | 7.76E+02 | 1.62E+04 | 1.25E+03 | 126 | 8.34E+03 | 59.17 | 1260.00 | 1.29E+01 | 7.76E+02 | 1.62E+04 | 1252.09 | 1253.51 | 2.02E+00 | 1260.00 | 0.63 | 4.36E+02 | -1.42E+02 | | |
| 1.70E+04 | 1.31E+03 | 1320.00 | 1.30E+01 | 7.77E+02 | 1.70E+04 | 1.31E+03 | 132 | 8.33E+03 | 59.17 | 1320.00 | 1.30E+01 | 7.77E+02 | 1.70E+04 | 1311.47 | 1312.81 | 1.79E+00 | 1320.00 | 0.65 | 4.93E+02 | 3.51E+02 | | |
| 1.78E+04 | 1.37E+03 | 1380.00 | 1.30E+01 | 7.77E+02 | 1.78E+04 | 1.37E+03 | 138 | 8.32E+03 | 59.18 | 1380.00 | 1.30E+01 | 7.77E+02 | 1.78E+04 | 1370.05 | 1372.07 | 4.08E+00 | 1380.00 | 0.72 | 5.54E+02 | 9.05E+02 | | |
| 1.85E+04 | 1.43E+03 | 1440.00 | 1.30E+01 | 7.78E+02 | 1.85E+04 | 1.43E+03 | 144 | 8.32E+03 | 59.18 | 1440.00 | 1.30E+01 | 7.78E+02 | 1.85E+04 | 1429.21 | 1431.28 | 4.30E+00 | 1440.00 | 0.75 | 6.22E+02 | 1.53E+03 | | |

**Figure-1.** Snap of excel data sheet for calculating dissipated energy.

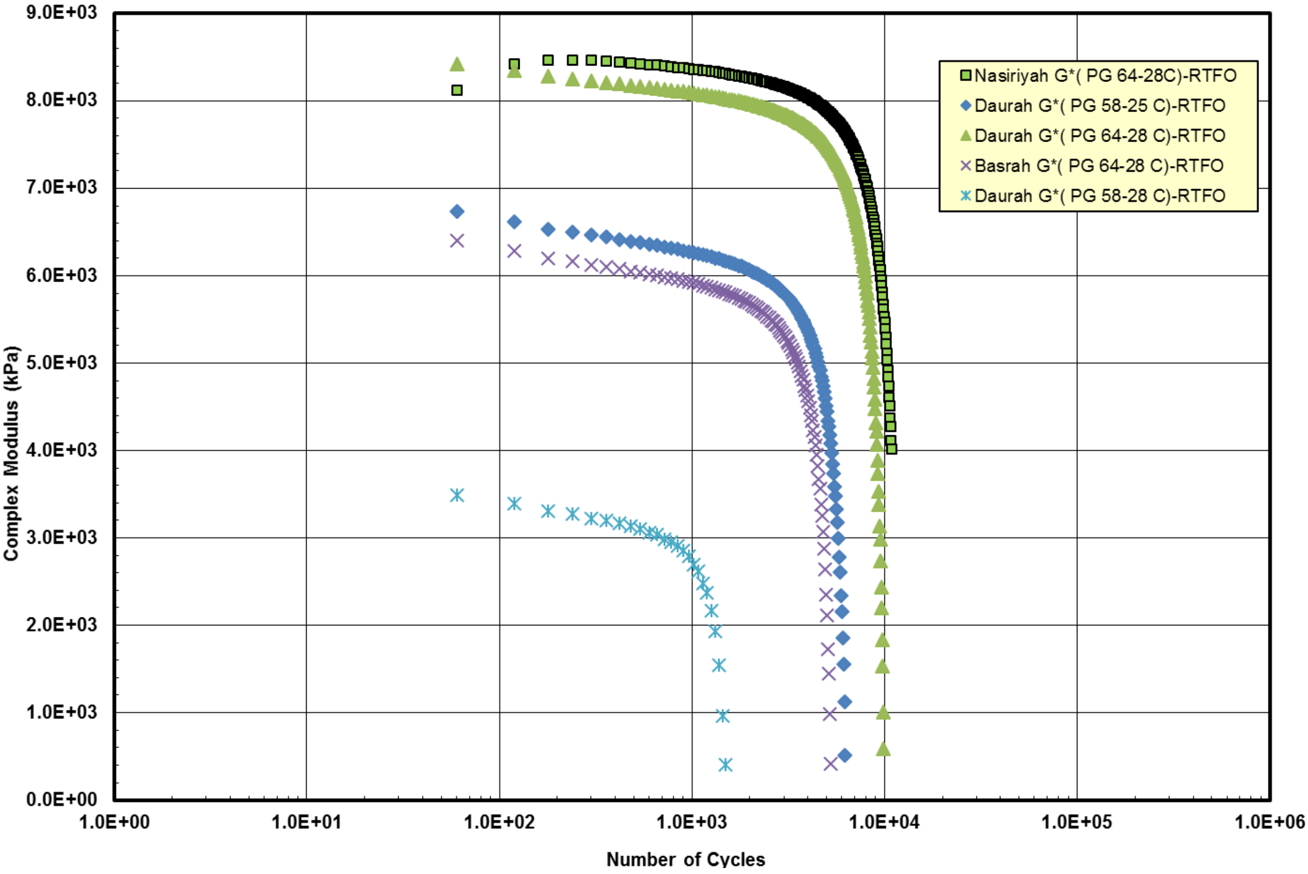


**Figure-2.** Binders Fatigue Results at 10Hz, Control Stress (200 kPa) and RTFO Aging.

ARPN Journal of Engineering and Applied Sciences
©2006-2019 Asian Research Publishing Network (ARPN). All rights reserved.
www.arpnjournals.com

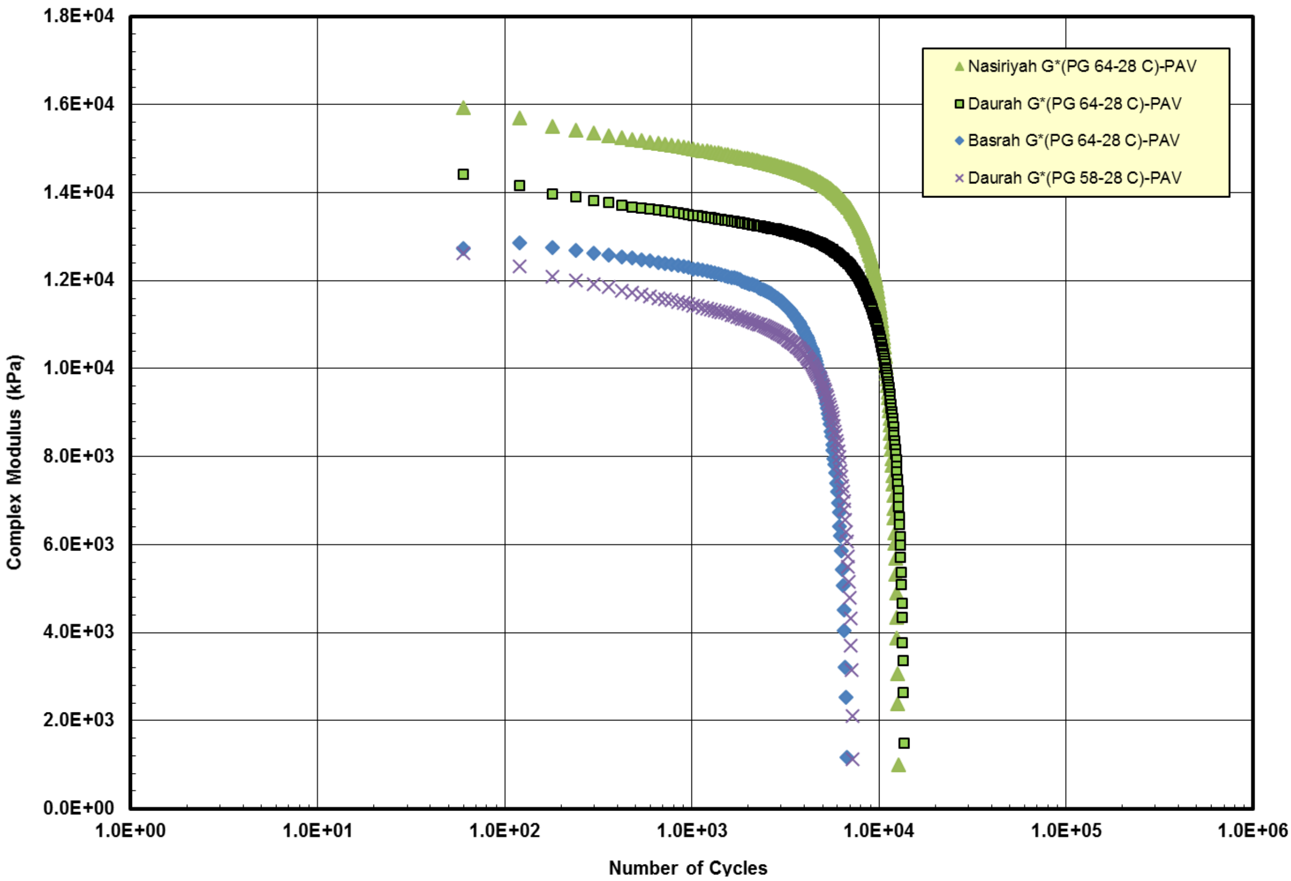


**Figure-3.** Binders Fatigue Results at 10 Hz, Control Stress (350 kPa) and PAV.

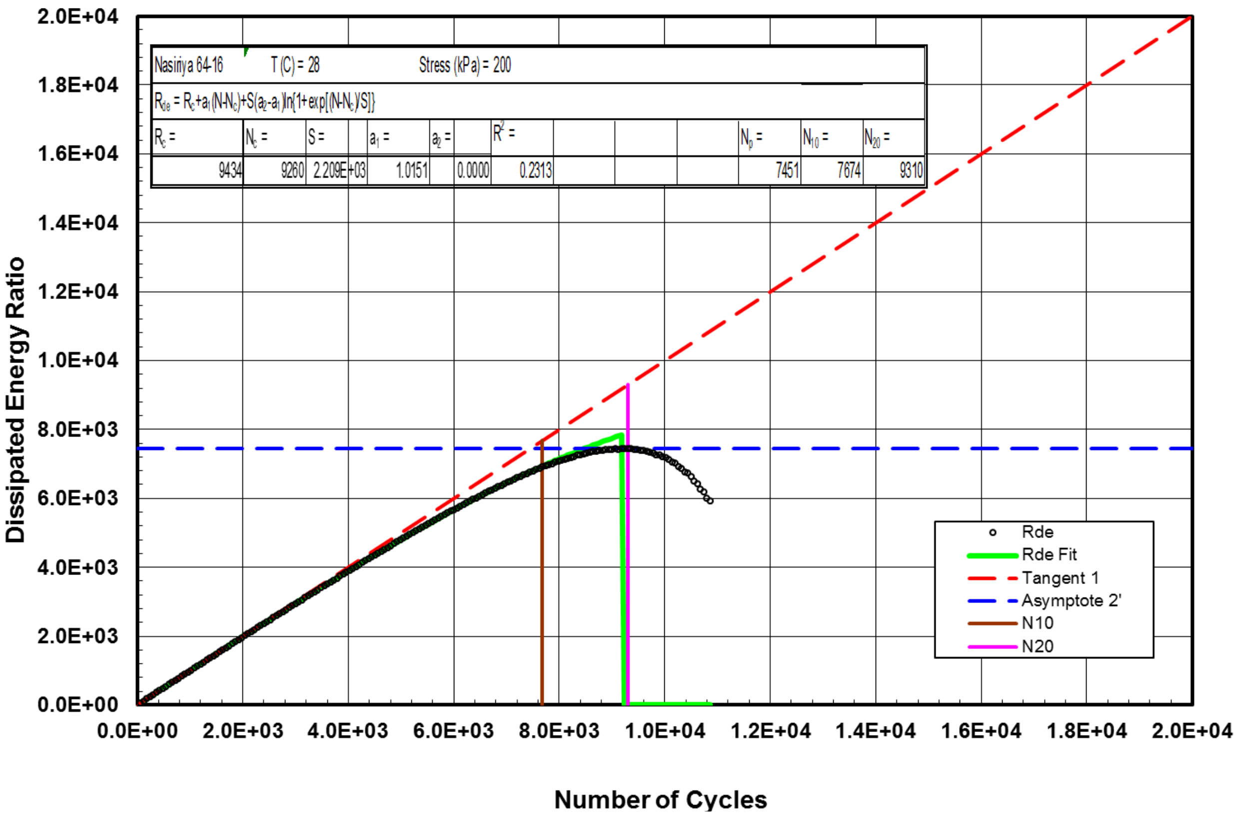


**Figure-4.** Typical Dissipated Energy Ratio with Fatigue Life at Control Stress (200 kPa) and 10 Hz.

ISSN 1819-6608
ARPN Journal of Engineering and Applied Sciences
©2006-2019 Asian Research Publishing Network (ARPN). All rights reserved.


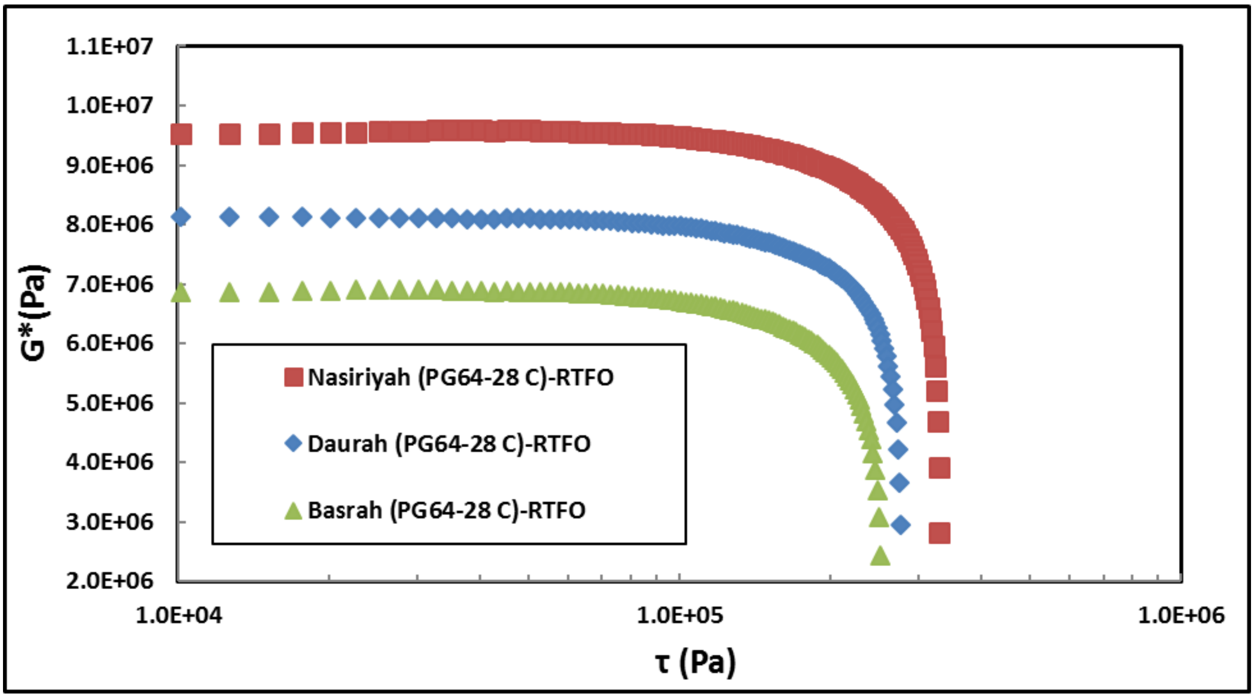


**Figure-5.** Resistance of Shear Modulus with Shear Stress for Local asphalt Binders at RTFO Aging.

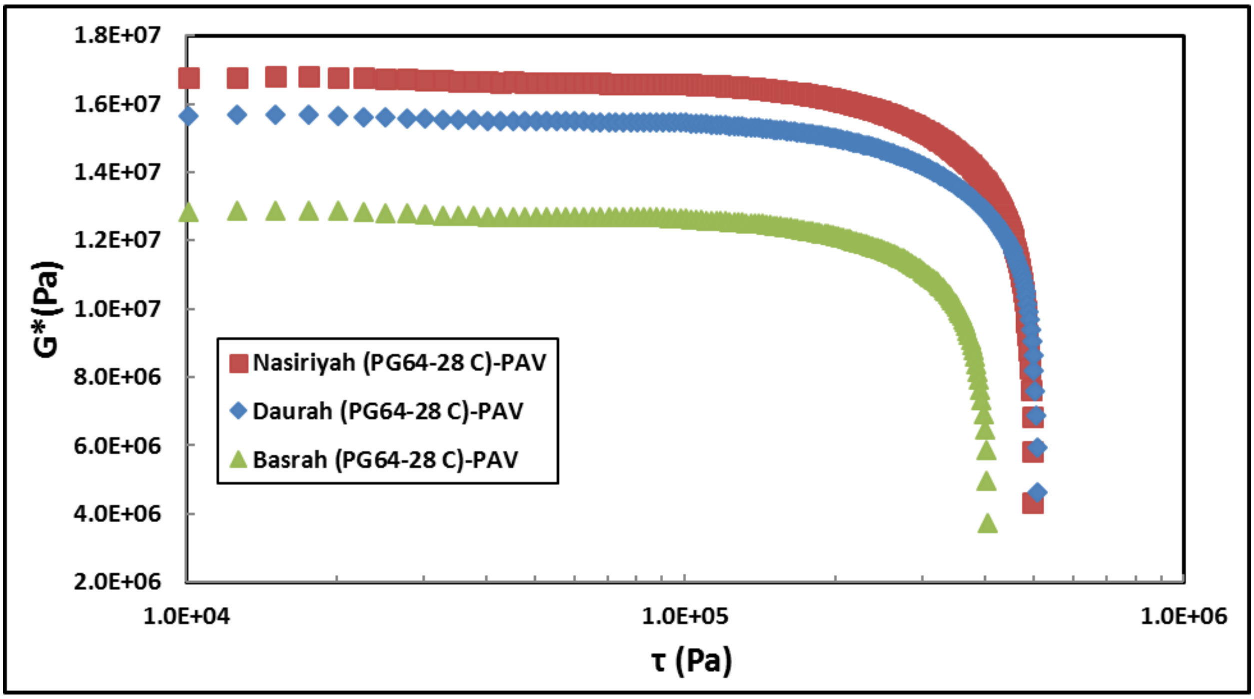


**Figure-6.** Resistance of Shear Modulus with Shear Stress for Local asphalt Binders at PAV Aging.

ARPN Journal of Engineering and Applied Sciences
©2006-2019 Asian Research Publishing Network (ARPN). All rights reserved.


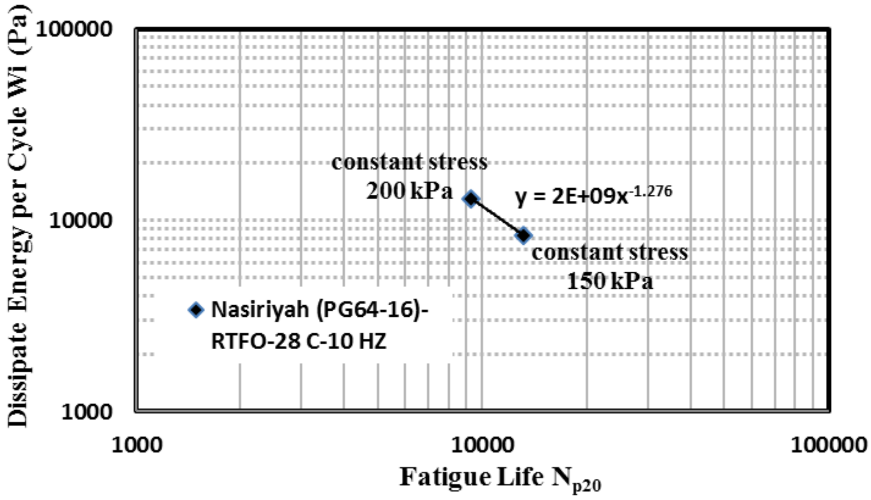


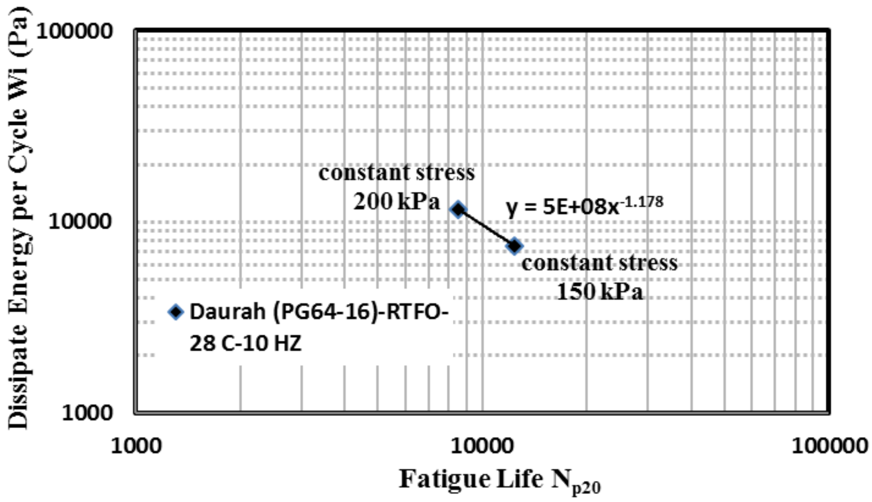


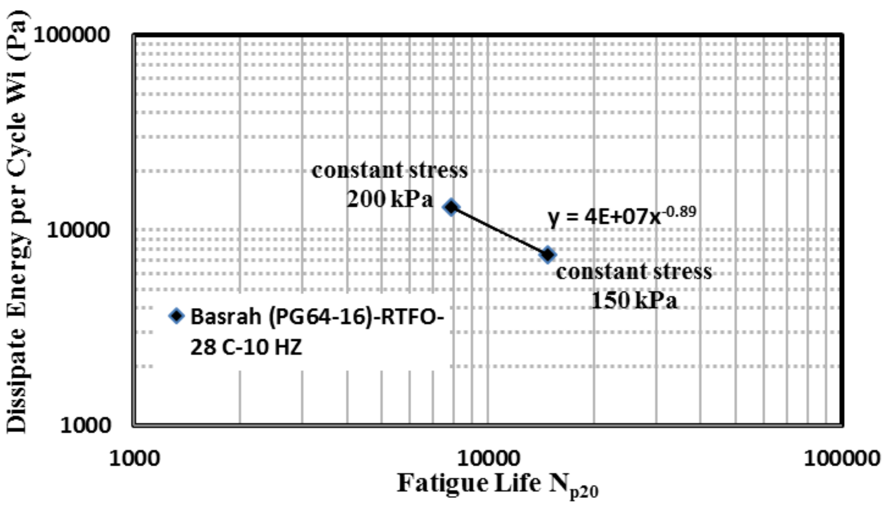


**Figure-7.** Modes of Fatigue life Failure for the Local asphalt Binders at RTFO Aging.

VOL. 14, NO. 7, APRIL 2019 ISSN 1819-6608
ARPN Journal of Engineering and Applied Sciences
©2006-2019 Asian Research Publishing Network (ARPN). All rights reserved.


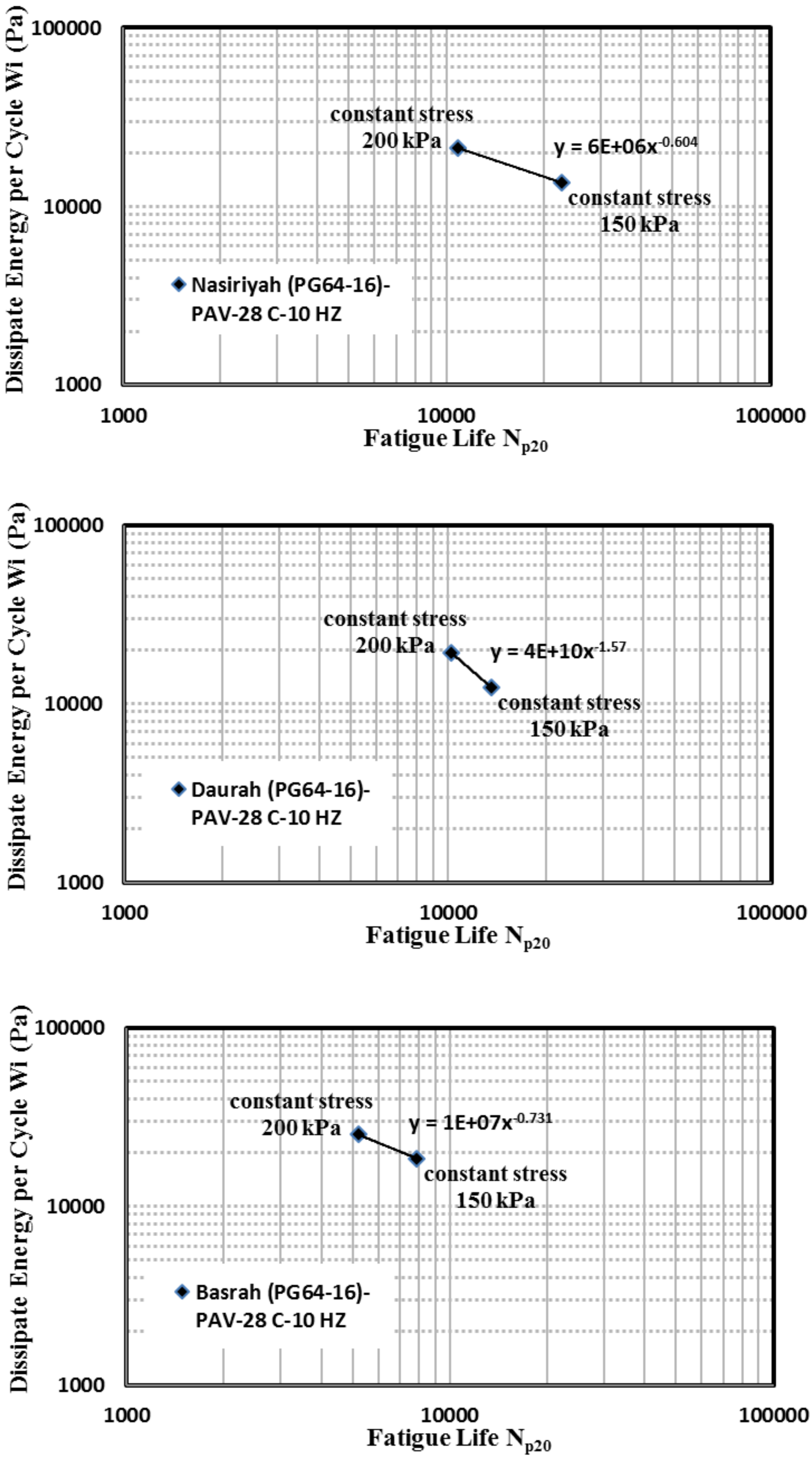


**Figure-8.** Modes of Fatigue life Failure for the Local asphalt Binders at PAV Aging.